Absence of renal hypoxia in the subacute phase of severe renal ischemia reperfusion injury

Connie P. C. Ow[1], Jennifer P. Ngo[1], Md Mahbub. Ullah[1], Giannie Barsha[1], Ruth C. Meex[2], Matthew J. Watt[3], Lucinda M. Hilliard[1], Maarten P. Koeners[4,5] and Roger G. Evans[1]

[1]Cardiovascular Disease Program and [3]Metabolism, Diabetes and Obesity Program, Biomedicine Discovery Institute, Department of Physiology, Monash University, Melbourne, Australia,[2]NUTRIM School of Nutritional and Translational Research in Metabolism, Maastricht University Medical Centre, Department of Human Biology, Maastricht, The Netherlands, [4]School of Physiology, Pharmacology and Neuroscience, Biomedical Sciences, University of Bristol, United Kingdom and [5]Institute of Biomedical and Clinical Science, University of Exeter Medical School, United Kingdom

Running title: Tissue oxygenation in renal ischemia reperfusion injury

Author for correspondence at current address:

Dr Connie Ow

Department of Cardiac Physiology

National Cerebral and Cardiovascular Center Research Institute

5-7-1 Fujishirodai, Suita-Shi, Osaka 565-8565 Japan

Tel: +81-6-6833-5012

Fax: +81-6-6835-5416

Email: ow.peichenconnie73@ncvc.go.jp

Abstract

Tissue hypoxia has been proposed as an important event in renal ischemia reperfusion injury (IRI), particularly during the period of ischemia and in the immediate hours following reperfusion. However, little is known about renal oxygenation during the subacute phase of IRI. We employed four different methods to assess the temporal and spatial changes in tissue oxygenation during the subacute phase (24 h and 5 days after reperfusion) of a severe form of renal IRI in rats. We hypothesized that the kidney is hypoxic 24 h and 5 days after an hour of bilateral renal ischemia, driven by a disturbed balance between renal oxygen delivery (DO_2) and oxygen consumption (VO_2). Renal DO_2 was not significantly reduced in the subacute phase of IRI. In contrast, renal VO_2 was 55% less 24 h, and 49% less 5 days after reperfusion than after sham-ischemia. Inner medullary tissue PO_2, measured by radiotelemetry was 25 ± 12% greater 24 h after ischemia than after sham-ischemia. By 5 days after reperfusion, tissue PO_2 was similar to that in rats subjected to sham-ischemia. Tissue PO_2 measured by Clark electrode was consistently greater 24 h, but not 5 days, after ischemia than after sham-ischemia. Cellular hypoxia, assessed by pimonidazole adduct immunohistochemistry, was largely absent at both time-points and tissue levels of hypoxia inducible factors were downregulated following renal ischemia. Thus, in this model of severe IRI, tissue hypoxia does not appear to be an obligatory event during the subacute phase, likely due to the markedly reduced oxygen consumption.

Word count: 249

Introduction

Acute kidney injury (AKI) is a major cause of death and disability globally and places a major acute burden on healthcare systems (26). It also renders patients more susceptible to later development of chronic kidney disease (CKD) (2). For example, a diagnosis of AKI was found to be associated with an 8.8 fold excess risk of later development of CKD (8). Furthermore, the risk of later development of CKD increases with the severity of AKI (8). Tissue hypoxia has been proposed as an important driver in the pathogenesis of both AKI and CKD, although this proposition remains to be definitively tested (33).

Ischemia reperfusion injury (IRI) sustained from medical interventions often arises from the obligatory need to restrict or completely prevent blood flow to the kidney, resulting in a period of severe hypoxia or complete anoxia (15). Cellular damage such as acute tubular necrosis and tubular apoptosis is evident during the reperfusion period and is likely driven in part by the presence of tissue hypoxia during the period of ischemia. In experimental IRI, cortical (27, 28, 41) and medullary (27, 28, 34) tissue hypoxia has also been observed during the first few hours of reperfusion after complete renal ischemia. Importantly, the kidney was observed to be hypoxic even with some level of, albeit incomplete, structural and functional recovery (3, 4). However, there are little available data regarding renal tissue oxygenation beyond the first few hours of reperfusion during the extension and recovery phase of IRI. This information is required if we are to understand the role of tissue hypoxia in the natural history of AKI, either as it progresses to end-stage renal disease or renal function recovers but the risk of later CKD is increased.

The chief aim of the current study was to assess the time-course of changes in, and the spatial distribution of, tissue oxygen tension (PO_2) during the subacute phase of severe IRI (the first 5 days of reperfusion after 60 min of bilateral renal ischemia). We chose severe IRI in an attempt to model the clinical situation of severe AKI leading to end-stage renal disease,

cognizant of the possibility that renal oxygenation in this scenario might differ considerably from that in milder forms of renal IRI. We tested the hypothesis that renal tissue is hypoxic during the subacute phase of IRI. Four approaches were used for assessment of renal tissue oxygenation, each with varying temporal and spatial resolution. Radiotelemetry was used to examine the time-course of changes in inner medullary tissue PO_2 in freely-moving rats (22, 23). Clark-type electrodes were used to characterize the spatial variations in renal tissue PO_2 in the renal cortex and medulla of anesthetized rats at both 24 h and 5 days after reperfusion. This experiment also provided an opportunity to determine the contribution of changes in renal oxygen delivery (DO_2) and oxygen consumption (VO_2) to alterations in renal tissue PO_2 24 h and 5 days after reperfusion. Pimonidazole adduct immunohistochemistry was used to characterize the spatial distribution of cellular hypoxia 24 h and 5 days after reperfusion. We also measured the expression of hypoxia-inducible factors (HIF-1α and HIF-2α) and some of their downstream gene targets.

Methods

Experimental Animals

Ten to twelve week old male, Sprague-Dawley rats (n=70) were obtained from the Animal Resources Centre (Perth, Western Australia). They were housed in a room maintained at 21–23 ºC with a 12 h light/dark cycle. The rats were allowed free access to water and standard laboratory rat chow. All procedures were approved in advance by the Animal Ethics Committee of the School of Biomedical Sciences, Monash University as being in accordance with the Australian Code of Practice for the Care and Use of Animals for Scientific Purposes.

Induction of bilateral renal ischemia

Rats were anesthetized with isoflurane (IsoFlo™, 05260-05, Abbott Laboratories, USA), using a vaporizer and maintained at 2.5 – 3.0% v/v. A midline incision was made to

expose the left and right renal arteries. To induce bilateral renal ischemia (n = 36), blood flow to both kidneys was prevented by the application of microvascular clamps (00398, S&T AG, Switzerland) placed on both the left and right renal arteries and veins. Complete ischemia was confirmed by observing the blanching of the kidneys. After an hour, the microvascular clamps were removed, so blood flow to both kidneys was restored. Wounds were closed in layers with sutures and each rat was then allowed to recover from the surgery on a heated pad for an hour. A separate cohort of rats (n = 34) underwent the same procedure with the exception of the application of the microvascular clamps and so served as controls (sham-ischemia). Rats received subcutaneous injections of an analgesic (carprofen, 1.25 mg, Pfizer, Australia) for two consecutive days following recovery from surgery.

Protocol 1: Temporal changes in renal tissue oxygenation following renal ischemia

We employed a radiotelemetric method (22, 23) to characterize the temporal profile of changes in renal tissue PO_2 after renal ischemia and reperfusion. Briefly, the oxygen telemeter was implanted under isoflurane anesthesia so that the tip of the oxygen-sensing carbon paste electrode was in the inner medulla of the left kidney (5 mm below the renal capsule). One week after implantation of the telemetric probe, the rats underwent a second surgical procedure for the induction of either bilateral renal ischemia (n = 7, body weight = 501 ± 20 g) or sham-ischemia (n = 5, body weight = 491 ± 21 g). Renal tissue PO_2 was recorded continuously for 1 day before and for 5 days after recovery from surgery. Rats received subcutaneous injections of an analgesic (carprofen, 1.25 mg, Pfizer, Australia) prior to laparotomy and for two consecutive days following recovery from surgery.

Measurements & Calculations: Current measured by the telemeters was filtered with a 25 Hz low-pass filter and artifactual measurements were removed when the 1^{st} order derivative of the measured current exceeded the threshold of 5-500 nA/s. The zero-offset current, acquired when the rat was killed at the end of the study via induction of cardiac arrest under anesthesia

(22), was determined and subtracted. Data are presented as a percentage of the average value on the day before surgery to induce ischemia or sham-ischemia.

Protocol 2: Renal tissue oxygenation and its determinants after renal ischemia

Either 24 h or 5 days following recovery from renal ischemia or sham-ischemia, rats were anesthetized and prepared for the assessment of regional tissue PO_2 using a Clark electrode (50 μm tip, OX-50, Unisense, Denmark). We assessed i) cortical tissue PO_2 across a range of sites on the dorsal surface of the kidney and ii) a profile of tissue PO_2 with depth from the cortical surface. In this set of studies, we also determined the major determinants of tissue PO_2, renal DO_2 and VO_2.

Rats (n = 6-11 per group) were anesthetized with sodium thiobutabarbital (100 mg/kg *i.p.,* Inactin; Sigma, St Louis, MO, USA). A tracheostomy was performed to facilitate artificial ventilation with 40% inspired oxygen at a ventilation rate of 90–100 breaths/min and a tidal volume of 3.5 ml (Ugo Basile, Model 7025, SDR Clinical Technology, NSW, Australia) as previously described (1). The left carotid artery was catheterized to facilitate arterial blood sampling and blood pressure measurement. The right jugular vein was catheterized to facilitate infusion of maintenance fluid (154 mM NaCl) at a rate of 6 ml/h during the period of surgical preparation. The bladder was catheterized, for collection of urine from the left kidney, for assessment of renal function using standard clearance methods. The degree of saturation of hemoglobin with oxygen was measured continuously using a sensor placed on the foot (Mouse Ox, Starr Life Sciences, Oakmont, PA, USA).

The right renal artery and vein were ligated and a catheter was passed from the right renal vein through the vena cava and into the left renal vein for the sampling of renal venous blood. Total renal blood flow (RBF) was measured using a transit-time ultrasound flow probe (Type 0.7 VB, Transonic Systems Inc., NY, USA) placed around the left renal artery. Following completion of the surgical preparations, rats received bolus doses of [^{3}H]-inulin

(10 μCi in 50 μl, Perkin Elmer Australia, Melbourne, Australia) and pancuronium bromide (2 mg/kg, Astra Zeneca Pty Ltd, NSW, Australia) intravenously. A maintenance infusion of 2% w/v bovine serum albumin (Sigma Aldrich, St Loius, MO, USA) in 154 mM sodium chloride delivered 676 nCi/h [^{3}H] inulin and 0.1 mg/kg/h pancuronium bromide through the jugular vein at a rate of 2 ml/h. The infusion commenced once all surgical preparations were completed and was maintained throughout the rest of the protocol.

After a 1 h equilibration period, a 0.5 ml sample of arterial blood was taken for blood oximetry. The plasma component of the sample was later used for assessment of the concentrations of [^{3}H]-inulin and sodium. A 0.1 ml sample of renal venous blood was also collected for blood oximetry. Renal tissue PO_2 was then assessed using a Clark electrode attached to a micromanipulator. Two series of measurements were taken. In the first series, the electrode was advanced 2 mm from the renal surface, into the cortex, at 6 randomly chosen sites across the left kidney. The second series established a profile of tissue PO_2 with depth below the cortical surface. The electrode was moved to the mid-point of the cortical surface of the kidney and advanced into the kidney at 1 mm increments up to a depth of 10 mm from the renal surface as previously described (32). Once all measurements were taken, a second set of blood samples, from the carotid artery and the renal vein, was taken as before. Urine made by the left kidney, during the period of measurement of tissue PO_2, was collected for measurement of the concentrations of [^{3}H]-inulin and sodium.

Measurements & Calculations: Arterial pressure, heart rate (triggered by arterial pressure), RBF, core body and tissue temperature and renal tissue PO_2 measured by Clark electrode were digitized as previously described (32). Urinary and plasma concentrations of sodium were determined using ion-sensitive electrodes (EasyElectrolytes, Medica Corporation, Bedford USA). Glomerular filtration rate (GFR) was determined by the clearance of [^{3}H]-inulin. Blood chemistry was assessed using a point-of-care device (iSTAT®, CG8+

cartridges, Abbott laboratories, Abbott Park, IL, USA). Arterial and venous blood oxygen content was calculated as previously described (1).

Protocol 3: Cellular hypoxia and hypoxic signaling after renal ischemia

Either after 24 h or 5 days of recovery from bilateral renal ischemia or sham - ischemia (n = 6 per group), rats were prepared for perfusion-fixation of the right kidney. In this set of studies, the chief aim was to assess cellular hypoxia using pimonidazole adduct immunohistochemistry. Pimonidazole chloride (HP1-1000Kit, Hydroxyprobe Inc., USA) was administered, at a dose of 60 mg/kg *i.p.* three hours before perfusion-fixation of the kidney.

Three hours after the injection of pimonidazole, rats were anesthetized with sodium pentobarbital (60 mg/kg, *i.p.*, Sigma Aldrich, MO, USA). The left carotid artery was catheterized to facilitate arterial blood sampling. A midline incision was then made exposing both kidneys and the bladder. A urine sample was taken by puncturing the bladder wall and was frozen at -20 °C for later analysis. The left renal artery and vein were isolated and freed from surrounding connective tissue and fat. Lidocaine (2% w/v; Xylocaine®, Astra Zeneca, NSW, Australia) was applied onto both vessels to prevent spasm of the renal artery. Silk ligatures (3/0 Dysilk, Dynek Pty Ltd, SA, Australia) were placed around the vena cava above the level of the right kidney, around the left renal artery and vein and around the abdominal aorta. An incision was made in the abdominal aorta below the level of the left kidney and a polyurethane catheter connected to the perfusion apparatus was advanced into the aorta, facing upstream, thereby facilitating retrograde perfusion. A 1 ml blood sample was taken from the carotid artery for later analysis. The left renal artery and vein were then ligated and the left kidney removed, decapsulated and snap frozen in liquid nitrogen for later analysis of HIF-1α and HIF-2α protein and gene expression of *HIF-1α, HIF-2α, VEGF-α and HO-1*. Prior to freezing, the left kidney was sectioned in the coronal plane into 4-5 slices of approximately 1–2 mm thickness.

The ligatures surrounding the vena cava and abdominal aorta were tied off and the right kidney perfused with 100–150 ml of 4% w/v paraformaldehyde (PFA, paraformaldehyde powder, no. 158127, Sigma-Aldrich) at room temperature and a pressure of 150 mmHg. The inferior vena cava was incised to vent perfusate. The perfused kidney was removed, decapsulated and stored in 4% PFA for 48 h before it was processed for embedding and staining at the Monash Histology Platform.

Blood chemistry was assessed using a point-of-care device (iSTAT®, CHEM8+ cartridges, Abbott laboratories). Urinary albumin concentration was determined using direct competitive enzyme linked immunosorbent assay (Nephrat II, NR 002, Exocell Inc., PA, USA). Urinary creatinine concentration was determined using an assay based on Jaffe's reaction of alkaline picrate solution with creatinine (Creatinine Companion, 1012 Strip Plate, Exocell Inc.).

Quantification of fibrosis. The right kidney was processed, embedded in paraffin and sectioned at a thickness of 5 μm in the coronal plane. Collagen deposition was assessed by staining with 1% w/v picrosirius red. The cortical, outer and inner medullary region of the kidney in each section was identified using Aperio Imagescope (Leica Biosystems Imaging Inc., Australia). The amount of collagen deposited was quantified as a percentage of the entire area in each region.

Pimonidazole adduct immunohistochemistry. Antigen retrieval was carried out by incubating the sections in citrate buffer (Target Retrieval Solution, DAKO, Australia) at 90 °C for 30 min. Sections were then washed in tris-buffered saline (154 mM NaCl) with Tween 20 (DAKO Australia) (TBST) once they had cooled to 80 °C. Excessive tissue peroxidase activity was then quenched using 0.03% v/v hydrogen peroxide containing sodium azide (DAKO, Denmark) for 10 min. Sections were then incubated in a protein block serum

(Protein Block Serum-free, DAKO, Australia) for 10 min, in order to remove non-specific binding, and washed twice more in TBST. Sections were then treated with an affinity purified polyclonal anti-pimonidazole antibody raised in the rabbit (1:200 dilution, PAb2627AP, Hydroxyprobe Inc.) for 1 h at room temperature before incubation in goat anti-rabbit secondary antibody conjugated with horseradish peroxidase (polyclonal goat EnVision, DAKO, Denmark) for 30 min at room temperature. Sections were washed twice with TBST before incubation with 3-diaminobenzidine (DAKO, Denmark) for 10 min and then counterstained with haematoxylin (DAKO, Automations Hematoxylin, USA) before being cover-slipped.

Western blot analysis of HIF-1α and HIF-2α proteins. The snap frozen kidney was thawed and the cortex, outer and inner medulla inclusive of the papilla were rapidly dissected. To stop further enzymatic reactions, the tissue samples were placed in 8 µl per mg of radioimmuno-precipitation assay (RIPA) buffer (consisting of 50 mM Tris-Hcl, 150 mM NaCl, 0.1% Triton X-100, 0.5% sodium deoxycholate, 0.1% sodium dodecylsulphate (SDS), 1 mM sodium orthovanadate, 1 mM NaF, 1:25 of 25x phosphatase inhibitor, 1:10 of 10x phosphostop and 1:1000 dithiothreitol). The tissues were then homogenized at 14,000 RPM at 4 °C for 20 min and equal amounts of protein (30 µg, determined by a Bradford protein assay) were loaded into a 7.5% pre-cast gel (7.5% Mini-Protean® TGX™ Precast Protein Gels, 4561025, Bio-Rad Laboratories, USA) and fractionated electrophoretically in Tris/Glycine/SDS running buffer at 300 V for 20 min. The fractionated protein in the gel was then transferred onto a nitrocellulose membrane (Bio-Rad Laboratories). Non-specific binding was blocked with 5% skim milk in TBST buffer. As the primary antibodies for HIF-1α (NB100-479, Novus Biologicals, LLC, CO, USA) and HIF-2α (NB100-122, Novus Biological LLC) are similar in molecular weight (115 and 118 kDa), we carried out the immunoblot analysis of each protein of interest on separate gels. The nitrocellulose

membranes were incubated overnight at 4 °C in the primary antibody (1:1000, raised in rabbit) made up in a solution of 2.5% w/v bovine serum albumin. The membranes were then incubated with 1:4000 secondary antibody (ECL™ anti-rabbit IgG, HRP-linked whole antibody, GE Healthcare UK Limited, UK) and 1:15,000 conjugate (Precision Protein™ StrepTactin-HRP conjugate, Bio-Rad Laboratories) for an hour at room temperature. The nitrocellulose membrane was developed using equal parts of Clarity™ Western Peroxide Reagent (Bio-Rad Laboratories) and Clarity™ Western Luminol/Enhancer Reagent (Bio-Rad Laboratories) for 3 min before imaging. The intensity of the bands observed on the membrane was quantified and corrected for variability in protein migration down the gel and for total protein content loaded into the wells. Comparisons were made between treatment groups across the two time points within each region (*i.e.* cortex, outer and inner medulla).

Quantitative real-time PCR. The tissue samples were homogenized and total RNA was isolated using the RNeasy Mini Kit (74104, Qiagen Inc., Australia). Pre-designed assays for primers of the 18s house keeping gene (Rn03928990_g1), *HIF-1α* (Rn01472831_m1), *HIF-2α* (Rn00576515_m1), *VEGF-α* (Rn01511602_m1) and *HO-1* (Rn00561387_m1) genes were obtained from ThermoFisher Scientific Inc. Real-time PCR was performed on ABI 7900 HT (ThermoFisher Scientific Inc., Australia). Data were calculated by the $2^{-\Delta\Delta Ct}$ method.

Statistical analysis

Statistical analyses were performed using the software package SYSTAT (Version 13, Systat Software, San Jose, CA). Two-sided $P \leq 0.05$ was considered statistically significant. Normality was assessed using the Shapiro-Wilk test (40). Data that did not violate normality are presented as mean ± standard error of the mean (SEM) while data that violated normality are presented as median (25th percentile, 75th percentile). Analysis of variance (ANOVA) was used to assess the independent effects of treatment and time and their

interaction. For data the violated normality, an ANOVA on ranking (9) was performed instead. Dichotomous comparisons of continuous variables were made using Student's t-test for data that did not violate normality and the Mann-Whitney U-test was performed for data that violated normality. To protect against the risk of type I error arising from multiple comparisons, P-values were conservatively adjusted using the Dunn-Sidak procedure (30). P-values derived from within-subjects factors in repeated measures ANOVA were conservatively adjusted using the method of Greenhouse and Geisser (31).

Results

Protocol 1: Temporal changes in renal tissue oxygenation following renal ischemia

On the first day after reperfusion, inner medullary tissue PO_2 measured by telemetry was 25 ± 12% greater than its control level (Day -1) (Fig. 1). Tissue PO_2 then gradually fell to be close to its control level by the fifth day after reperfusion of the kidney. After sham-ischemia, inner medullary tissue PO_2 tended to gradually fall, so was 22 ± 11% less than its control level by day five after surgery.

Protocol 2: Renal tissue oxygenation and its determinants after renal ischemia

Systemic parameters. Twenty-four hours after reperfusion, body weight did not differ significantly from that of rats that underwent sham-ischemia. By 5 days after renal ischemia, rats had lost 39.2 ± 6.1 g of their body weight. Left kidney weight 24 h after renal ischemia was similar to that after sham-ischemia. In contrast, left kidney weight was 56% greater 5 days following renal ischemia than after sham-ischemia (Table 1). Mean arterial pressure was similar in the two groups of rats at both 24 h and 5 days after surgery.

Renal tissue oxygenation. Tissue PO_2 in the renal cortex was highly heterogenous, both 24 h and 5 days after either ischemia or sham-ischemia (Fig. 2A). Cortical PO_2 was, on average, 40% greater 24 h following renal ischemia than after sham-ischemia. By five days after renal ischemia, cortical tissue PO_2 was 39% less than 24 h after ischemia and similar to that in rats

subjected to sham-ischemia five days previously (Fig. 2B). Tissue PO_2 varied little with depth from the cortical surface. At 24 h after reperfusion, tissue PO_2 tended to be greater in rats subjected to ischemia than those subjected to sham-ischemia, the difference reaching statistical significance at depths of 5 mm (inner medulla), and 9 and 10 mm (cortex) (Fig. 2C). Five days after renal ischemia tissue PO_2 did not differ significantly from its level in rats subjected to sham-ischemia, at any depth below the cortical surface (Fig. 2D).

Renal hemodynamics and function. Renal blood flow was not significantly different in rats subjected to ischemia, compared with rats subjected to sham-ischemia, both 24 h and 5 days after surgery (Table 2). Twenty-four hours after ischemia, mean GFR (-99%), urine flow (-82%) and sodium excretion (-85%) were less than in after sham-ischemia (Table 2). Fractional excretion of sodium did not differ significantly 24 h after ischemia compared to sham-ischemia. By five days after ischemia, renal function was highly variable between rats, with some rats having recovered relatively normal GFR while others remained in apparent renal failure. Consequently, none of these variables differed significantly from their level in rats subjected to sham-ischemia. We were unable to detect a significant correlation ($r^2 = 0.03$, n=8), in rats subjected to ischemia, between GFR and tissue PO_2 at day 5 after surgery.

Blood oximetry and renal oxygen consumption and delivery. Arterial blood hematocrit 24 h after renal ischemia was 12% less than after sham-ischemia (Table 1). We were unable to detect a significant correlation (r^2=0.034, n=9), in rats subjected to ischemia, between hematocrit and tissue PO_2 24 h after reperfusion. By 5 days after renal ischemia, hematocrit was similar in the two groups of rats. Arterial blood PO_2 was 22% less, and SO_2 2.7% less, in rats 24 h after renal ischemia than after sham surgery. Renal DO_2 tended to be (29%) less 24 h after renal ischemia than sham-ischemia, although this apparent effect was not statistically significant (P = 0.06). There was no significant difference in renal DO_2 5 days after surgery. When both time points were considered together (24 h and 5 days), renal VO_2 was 55% less

in rats subjected to ischemia than in those subjected to sham surgery. The fractional extraction of oxygen did not differ significantly between the treatments at either time-point.

Protocol 3: Cellular hypoxia and hypoxic signaling after renal ischemia

Pimonidazole adduct immunohistochemistry. No pimonidazole adducts were detected in tissues from rats that did not receive pimonidazole chloride or in sections that were not incubated with the primary antibody (data not shown). Kidney sections from sham operated rats appeared morphologically normal (Fig. 3 & 4). Pimonidazole adducts were largely absent in the cortical region of rats 24 h following sham-ischemia. However, there was diffuse staining of pimonidazole adducts in tubular elements of the outer and inner medulla following sham-ischemia. Kidney sections from rats 24 h following recovery from renal ischemia showed relatively little staining for pimonidazole adducts across all regions of the kidney, but some diffuse staining was present 5 days following ischemia and reperfusion. However, luminal aspects of tubules were often stained positive for pimonidazole adducts after renal ischemia, suggestive of marked tubular obstruction. There was significant cellular sloughing and disintegration of the brush border/apical membrane of tubules after renal ischemia. In addition, there were considerable cellular debris in the luminal aspects of tubules at 24 h after renal ischemia. Tubular profiles surrounding the debris-riddled tubules were often flattened. In contrast, tubules appeared to be mostly dilated 5 days after renal ischemia. By 5 days after ischemia, tubules in the cortex, outer and inner medulla appeared to be more dilated than after sham-ischemia or 24 h after renal ischemia.

HIF-1α and HIF-2α proteins. When both the 24 h and 5 day time-points were considered collectively, the expression of HIF-1α protein in the cortex, outer medulla and inner medulla was less after renal ischemia than after sham-ischemia (Fig. 5A-C). However, not all comparisons at individual time-points were statistically significant. HIF-1α levels in the cortex were 88.3% less 5 days after renal ischemia than at the corresponding time-point after

sham-ischemia (Fig. 5A). Similarly, in the outer medulla, HIF-1α was 62.2% less 24 h after renal ischemia and 79.7% less 5 days after renal ischemia than after sham surgery (Fig. 5B). In contrast, in the inner medulla, levels of HIF-1α protein did not differ significantly, between rats subjected to ischemia compared to those subjected to sham-ischemia, at either the 24 h or 5 day time-point (Fig. 5C). When both the 24 h and 5 day time points were considered collectively, the expression of HIF-2α protein was markedly less, in rats subjected to ischemia compared to those subjected to sham-ischemia, in the cortex and the outer medulla but not in the inner medulla. The level of HIF-2α in the cortex was 86.9% less 5 days after ischemia than after sham-ischemia (Fig. 5D). In the outer medulla of rats subjected to renal ischemia, HIF-2α expression was 55% less 24 h and 89.2% less 5 days after ischemia, than after sham-ischemia (Fig. 5E). The deficits in HIF-1α and HIF-2α in rats subjected to renal ischemia did not diminish between the 24 h and 5 day time points, if anything, becoming more marked (Fig. 5).

Expression of genes for HIF-1α, HIF-2α, VEGF-α and HO-1. There were no significant differences in the expression of mRNA for *HIF-1α, HIF-2α* or *VEGF-α*, either 24 h or 5 days following renal ischemia compared to after sham-ischemia (Fig. 6). The expression of *HO-1* tended to be greater after ischemia than after sham-ischemia, although this apparent effect was only statistically significant at the 5 day time-point.

Collagen deposition. Twenty-four hours after renal ischemia, picrosirius red staining did not differ significantly, from that seen in rats subjected to sham-ischemia, in either the cortex or the outer medulla. However, it was 43% less in the inner medulla (Fig. 7). By 5 days after renal ischemia, picrosirius red staining was 50% greater in the cortex of rats subjected to ischemia than those subjected to sham-ischemia. There was an apparent effect of the duration of recovery period on picrosirius red staining, which in the cortex and inner medulla was significantly greater 5 days after ischemia or sham-ischemia than at the 24 h time point.

Indices of renal dysfunction. The plasma concentrations of urea and creatinine, and the urinary albumin-creatinine ratio were all greater in rats after ischemia than after sham-ischemia (Fig. 8). These effects were statistically significant at the individual time points with the exception of urinary albumin to creatinine ratio 24 h after ischemia, where sufficient urine for analysis could only be generated from two animals.

Discussion

We determined the time-course of changes in, and the spatial distribution of, renal tissue PO_2 during the subacute phase of severe renal IRI. Using four different methods for assessing renal tissue oxygenation, we could not detect tissue hypoxia during the extension/recovery phase of IRI. Indeed, if anything, there was relative hyperoxia up to 48 h after an hour of bilateral renal ischemia. We also observed downregulation of the abundance of HIF-1α and HIF-2α protein, particularly in the cortex and outer medulla, both 24 h and 5 days after reperfusion. The apparent absence of renal hypoxia is consistent with the pattern of changes in renal DO_2 and VO_2 after ischemia and reperfusion. That is, RBF was relatively normal but there was a marked reduction in sodium reabsorption, and so presumably oxygen utilization for sodium reabsorption, at both 24 h and 5 days after reperfusion. When both time-points were considered together, renal VO_2 was significantly less, and DO_2 tended to be less, in rats subjected to ischemia than in those subjected to sham-ischemia. Thus, tissue PO_2 appears to be well maintained during the extension/recovery phase of severe renal IRI because changes in renal DO_2 and VO_2 are relatively balanced.

The methods we used to assess renal oxygenation have both strengths and weaknesses (11, 33). Radiotelemetry allows continuous measurement of renal tissue PO_2 in the absence of confounding effects of anesthesia (22, 23). However, tissue PO_2 can only be expressed in relative terms and can be measured at only one site in each animal. Clark electrodes allow generation of a spatial map of tissue PO_2, but only in anesthetized animals

(11, 33). Furthermore, it is not possible to resolve tissue PO_2 to the level of specific vascular and tubular elements, except in the superficial cortex (43). In addition, as we have found previously with Clark electrodes inserted into renal tissue from the dorsal surface of the kidney (32), the steep cortico-medullary gradient in tissue PO_2 generated in many previous studies (6, 10, 29) is not obviously evident. We have no adequate explanation for this, although it may relate to our use of relatively large electrodes (50 μm) or the angle of entry to the renal tissue, from the dorsal surface of the kidney, as a consequence of which the tip of the electrode does not enter the renal papilla. Pimonidazole adduct immunohistochemistry allows detection of cells with $PO_2 < 10$ mmHg but does not provide a quantitative measure of tissue PO_2 (37). Furthermore, as we found in the current study and previously (1), it is prone to artifactual staining of cellular debris and casts within damaged tubules. Quantification of the abundance of HIF-1α and HIF-2α protein provides information about the state of hypoxia signaling pathways. However, factors other than tissue PO_2 contribute to the regulation of HIF signaling (16). Thus, interpretation of our failure to detect hypoxia by any one of these methods would merit caution. However, the fact that our observations were consistent across the four methods provides compelling evidence that, at least in this severe form of IRI, tissue hypoxia is not an obligatory characteristic of the period from 24 h to 5 days after severe renal ischemia and reperfusion.

The most likely explanation for the absence of hypoxia 24 h and 5 days after reperfusion, and even increased tissue PO_2 at 24 h, is reduced sodium reabsorption and thus renal VO_2. In the rats we studied, the deficit in sodium reabsorption 24 h after ischemia and reperfusion could be attributed to the decreased filtered load of sodium. This appears to drive downregulation of Na^+-K^+-ATPase activity. For example, in response to severe renal ischemia (*i.e.* 60 min), the abundance (and activity) of basolateral Na^+-K^+-ATPase pumps, the apical Na-K-2Cl and the thiazide-sensitive Na^+-Cl^- cotransporters was shown to be greatly

433 reduced (25). But the magnitude of the apparent reduction in renal VO_2 we observed was
434 considerably less than the magnitude of the reduction in sodium reabsorption. For example,
435 sodium reabsorption was less than 1% of rats subjected to sham-ischemia, while VO_2 was
436 34% that of rats subjected to sham-ischemia 24 h after reperfusion. These observations are
437 consistent with the concept that oxygen utilization for sodium reabsorption becomes less
438 efficient in AKI. In support of this concept, Redfors and colleagues studied renal oxygen
439 utilization in patients with AKI subsequent to cardiothoracic surgery (35). They found a
440 deficit in sodium reabsorption of 59% in patients with AKI after cardiothoracic surgery
441 compared to patients without AKI (35). In contrast, renal VO_2 was similar in the two groups
442 of patients. Furthermore, renal VO_2 per unit of reabsorbed sodium was 2.4 times greater in
443 patients with AKI than in those without AKI (35). The inefficiency of oxygen utilization for
444 sodium reabsorption in AKI appears to be driven by multiple factors, including loss of
445 polarity of Na^+-K^+-ATPase pumps, oxidative stress and reduced bioavailability of nitric oxide
446 (17, 24).

447 Renal tissue PO_2 is determined by the balance between local DO_2 and VO_2 (12).
448 Thus, tissue PO_2 during recovery from AKI is likely to be model-dependent. In a model of
449 severe AKI such as the one used in the current study, in which the filtered load of sodium
450 (and thus oxygen utilization for sodium reabsorption) is greatly reduced but renal blood flow
451 (and thus presumably local tissue DO_2) is well preserved, the absence of tissue hypoxia, and
452 even tissue hyperoxia, might be expected. On the other hand, tissue hypoxia might be
453 predicted in a model of less severe renal dysfunction, and thus better preserved GFR. This
454 concept is consistent with clinical observations in patients after renal transplantation. Using
455 blood oxygen level-dependent magnetic resonance imaging (BOLD-MRI), Sadowski and
456 colleagues observed greater renal medullary oxygenation in patients with acute allograft
457 rejection than in patients with normal functioning allografts, despite the former having a

deficit in renal medullary perfusion (38). Similarly, Rosenberger and colleagues observed low HIF-1α abundance in biopsies of patients with non-functional allografts, but induction of HIF-1α in biopsies from functional grafts (36). Thus, there is a strong rationale for the methods used in the current study to be applied to a less severe model of AKI, in which tissue hypoxia might be more likely to occur.

It is noteworthy that HIF-1α and HIF-2α protein expression was downregulated not just at 24 h after reperfusion, presumably driven in part by increased tissue oxygen availability, but also 5 days after reperfusion, when tissue PO_2 was similar in rats exposed to ischemia and sham-ischemia. Inhibition of HIF-1α and HIF-2α abundance appears to be mediated by post-translational processes at both 24 h and 5 days after reperfusion, since the expression of mRNA for these proteins was relatively normal at both time-points. The bioavailability of HIFs is influenced by various factors, such as their phosphorylation (20), and hydroxylation of proline and asparagine residues on HIFs (44) that target these protein for ubiquitinylation. The levels of proline hydroxylases (PHDs) have been shown to be unaltered following ischemia and reperfusion of the kidney (13, 39). A caveat to that is the post-translational modification of HIFs by PHDs in the kidney is likely complex given that the expression patterns, and thus sensitivity, of PHDs varies in different regions of the kidney likely because of the heterogeneity of renal tissue PO_2 under physiological conditions (39). It is also noteworthy that mRNA for VEGF-α and HO-1, genes under the control of the HIF-1α and HIF-2α promoter, were not downregulated at 24 h or 5 days after reperfusion. This observation is consistent with the concept that factors other than HIFs regulate expression of these genes in the subacute phase of severe IRI. The signaling pathway for VEGFs is complex and is critical for neo-vascularization. A myriad of factors apart from HIFs, such as VEGF receptor signaling complexes and neurolipin, are able to modulate the abundance and activity of VEGFs (21). Kanellis and colleagues showed that expression of VEGF was unaltered in

response to ischemia reperfusion of the kidney (18). Interestingly, the expression of VEGF receptor 2 was increased following ischemia and VEGF was redistributed to the basolateral membrane, consistent with the established role of VEGF in the maintenance of an adequate blood supply, in remaining viable tissues, as evinced in the current study by relatively well maintained renal blood flow (19). Nevertheless, the permanent loss of peritubular capillaries, due to inadequate vascular reparation and/or neo-vascularization, appears to be an important event in the progression from ischemia-induced AKI to CKD (2, 4).

Perspectives & Significance

In models of AKI induced by complete renal ischemia, hypoxia during the period of ischemia is obligatory and is likely one of the drivers of necrosis and apoptosis associated with the development of AKI after reperfusion. Furthermore, other important factors during reperfusion, such as oxidative stress (5, 7) and influx of immune-modulatory cells (14, 42) are initiated, at least partly, by the hypoxia during ischemia. In the first few hours after reperfusion (acute phase), reduced renal tissue or microvascular PO_2 has been observed in some (27, 28) but not all (1) cases. To the best of our knowledge, our current report describes the first detailed investigation of tissue oxygenation during the subacute phase of renal IRI. We provide compelling evidence that, at least in severe IRI modeling subacute and end stage renal disease, renal tissue hypoxia is not present 24 h and 5 days after reperfusion. It is possible that the absence of hypoxia at these time-points in this experimental model of severe IRI is a consequence of the degree of renal damage and the consequent deficit in renal oxygen consumption. Thus, future studies should focus on less severe models of AKI and follow animals for longer periods after reperfusion, to better characterize the natural history of renal oxygenation during progression from AKI to CKD.

Grants

This work was supported by grants from the National Health and Medical Research Council of Australia (GNT606601 & GNT1024575). M.P.K is supported by the British Heart Foundation (FS/14/30630) and the European Union, Seventh Framework Programme, Marie Curie Actions (CARPEDIEM No 612280 and International Outgoing Fellowship No. 282821). M. J. W. is supported by the National Health and Medical Research Council of Australia (GNT1077703).

References

1. **Abdelkader A, Ho J, Ow CPC, Eppel GA, Rajapakse NW, Schlaich MP, and Evans RG**. Renal oxygenation in acute renal ischemia-reperfusion injury. *Am J Physiol Renal Physiol* 306: F1026-F1038, 2014.
2. **Basile DP, Bonventre JV, Mehta RL, Nangaku M, Unwin R, Rosner MH, Kellum JA, and Ronco C**. Progression after AKI: Understanding maladaptive repair processes to predict and identify therapeutic treatments. *J Am Soc Nephrol* 27: 687-697, 2016.
3. **Basile DP, Donohoe DL, Roethe K, and Mattson DL**. Chronic renal hypoxia after acute ischemic injury: Effects of L-arginine on hypoxia and secondary damage. *Am J Physiol Renal Physiol* 284: F338-F348, 2003.
4. **Basile DP, Donohoe DL, Roethe K, and Osborn JL**. Renal ischemic injury results in permanent damage to peritubular capillaries and influences long-term function. *Am J Physiol Renal Physiol* 281: F887-F899, 2001.
5. **Basile DP, Leonard EC, Beal AG, Schleuter D, and Friedrich JL**. Persistant oxidative stress following renal ischemia-reperfusion injury increases ANG II hemodynamic and fibrotic activity. *Am J Physiol Renal Physiol* 302: F1494-F1502, 2012.
6. **Baumgartl H, Leichtweiss HP, Lubbers DW, Weiss C, and Huland H**. The oxygen supply of the dog kidney: Measurements of intrarenal pO_2. *Microvasc Res* 4: 247-257, 1972.
7. **Chatterjee PK, Cuzzocrea S, Brown PAJ, Zacharowski K, Stewart KN, Morta-Filipe H, and Thiemermann C**. Tempol, a membrane-permeable radical scavenger, reduces oxidant stress-mediated renal dysfunction and injury in the rat. *Kidney Int* 58: 658-673, 2000.
8. **Coca SG, Singanamala S, and Parikh CR**. Chronic kidney disease after acute kidney injury: A systematic review and meta-analysis. *Kidney Int* 81: 442-448, 2012.
9. **Conover WJ, and Iman RL**. Rank transformation as a bridge between parametric and nonparametric statistics. *Am Stat* 35: 124-129, 1981.
10. **Epstein FH, Agmon Y, and Brezis M**. Physiology of renal hypoxia. *Annals New York Academy Of Sciences* 718: 72 - 82, 1994.
11. **Evans RG, Gardiner BS, Smith DW, and O'Connor PM**. Methods for studying the physiology of kidney oxygenation. *Clin Exp Pharmacol Physiol* 35: 1405-1412, 2008.
12. **Evans RG, Ince C, Joles JA, Smith DW, May CN, O'Connor PM, and Gardiner BS**. Hemodynamic influences on kidney oxygenation: Clinical implications of integrative physiology. *Clin Exp Pharmacol Physiol* 40: 106-122, 2013.
13. **Fang Y, Zhang H, Zhong Y, and Ding X**. Prolyl hydroxylase 2 (PHD2) inhibition protects human renal epithelial cells and mice kidney from hypoxia injury. *Oncotarget* 7: 54317-54328, 2016.
14. **Friedewald J, and Rabb H**. Inflammatory cells in ischemic acute renal failure. *Kidney Int* 66: 486-491, 2004.
15. **Fu Q, Colgan SP, and Shelley CS**. Hypoxia: the force that drives chronic kidney disease. *Clin Med Res* 14: 15-39, 2016.
16. **Haase VH**. Hypoxia-inducible factors in the kidney. *Am J Physiol Renal Physiol* 291: F271-F281, 2006.
17. **Hansell P, Welch WJ, Blantz RC, and Palm F**. Determinants of kidney oxygen consumption and their relationship to tissue oxygen tension in diabetes and hypertension. *Clin Exp Pharmcol Physiol* 40: 123-127, 2013.
18. **Kanellis J, Mudge SJ, Fraser S, Katerelos M, and Power DA**. Redistribution of cytoplasmic VEGF to the basolateral aspect of renal tubular cells in ischemia-reperfusion injury. *Kidney Int* 57: 2445-2456, 2000.

19. **Kanellis J, Paizis K, Cox AJ, Stacker SA, Gilbert RE, Cooper ME, and Power DA**. Renal ischemia-reperfusion increases endothelial VEGFR-2 without increasing VEGF or VEGFR-1 expression. *Kidney Int* 61: 1696-1706, 2002.
20. **Kietzmann T, Mennerich D, and Dimova EY**. Hypoxia-inducible factors (HIFs) and phosphorylation: Impact on stability, localization, and transactivity. *Front Cell Dev Biol* 4: 11, 2016.
21. **Koch S, and Claesson-Welsh L**. Signal transduction by vascular endothelial growth factor receptors. *Cold Spring Harb Perspect Med* 2: a006502, 2012.
22. **Koeners MP, Ow CPC, Russell DM, Abdelkader A, Eppel GA, Ludbrook J, Malpas SC, and Evans RG**. Telemetry-based oxygen sensor for continuous monitoring of kidney oxygenation in conscious rats. *Am J Physiol Renal Physiol* 304: F1471-F1480, 2013.
23. **Koeners MP, Ow CPC, Russell DM, Evans RG, and Malpas SC**. Prolonged and continuous measurement of kidney oxygenation in conscious rats. *Methods Mol Biol* 1397: 93-111, 2016.
24. **Kwon O, Corrigan G, Myers BD, Sibley R, Scandling JD, Dafoe D, Alfrey E, and Nelson WJ**. Sodium reabsorption and distribution of Na^+/K^+-ATPase during postischemic injury to the renal allograft. *Kidney Int* 55: 963-975, 1999.
25. **Kwon T-H, Frokiaer J, Han JS, Knepper MA, and Nielsen S**. Decreased abundance of major Na^+ transporters in kidneys of rats with ischemia-induced acute renal failure. *Am J Physiol Renal Physiol* 278: F925-F939, 2000.
26. **Lameire N, Bagga A, Cruz D, De Maeseneer J, Endre Z, Kellum J, Liu K, Mehta R, Pannu N, Van Biesen W, and Vanholder R**. Acute kidney injury: An increasing global concern. *Lancet* 382: 170-179, 2013.
27. **Legrand M, Almac E, Mik EG, Johannes T, Kandil A, Bezemer R, Payen D, and Ince C**. L-NIL prevents renal microvascular hypoxia and increase of renal oxygen consumption after ischemia-reperfusion in rats. *Am J Physiol Renal Physiol* 296: F1109-F1117, 2009.
28. **Legrand M, Kandil A, Payen D, and Ince C**. Effects of sepiapterin infusion on renal oxygenation and early acute renal injury after suprarenal aortic clamping in rats. *J Cardiovasc Pharmacol* 58: 192-198, 2011.
29. **Lübbers DW, and Baumgartl H**. Heterogeneities and profiles of oxygen pressure in brain and kidney as examples of the PO2 distribution in the living tissue. *Kidney Int* 51: 372-380, 1997.
30. **Ludbrook J**. On making multiple comparisons in clinical and experimental pharmacology and physiology. *Clin Exp Pharmcol Physiol* 18: 379-392, 1991.
31. **Ludbrook J**. Repeated measurements and multiple comparisons in cardiovascular research. *Cardiovasc Res* 28: 303-311, 1994.
32. **Ow CPC, Abdelkader A, Hilliard LM, Phillips JK, and Evans RG**. Determinants of renal tissue hypoxia in a rat model of polycystic kidney disease. *Am J Physiol Regul Integr Comp Physiol* 307: R1207-R1215, 2014.
33. **Ow CPC, Ngo JP, Ullah MM, Hilliard LM, and Evans RG**. Renal hypoxia in kidney disease: Cause or consequence? *Acta Physiol* 222: e12999, 2018.
34. **Pohlmann A, Hentschel J, Fechner M, Hoff U, Bubalo G, Arakelyan K, Cantow K, Seeliger E, Flemming B, Waiczies H, Waiczies S, Schunck W-H, Dragun D, and Niendorf T**. High temporal resolution parametric MRI monitoring of the initial ischemia/reperfusion phase in experimental acute kidney injury. *PLoS One* 8: e57411, 2013.
35. **Redfors B, Bragadottir G, Sellgren J, Sward K, and Ricksten S**. Acute renal failure is NOT an "acute renal success" - A clinical study on the renal oxygen supply/demand relationship in acute kidney injury. *Crit Care Med* 38: 1695-1701, 2010.

36. **Rosenberger C, Pratschke J, Rudolph B, Heyman SN, Schindler R, Babel N, Eckardt K-U, Frei U, Rosen S, and Reinke P**. Immunohistochemical detection of hypoxia-inducible factor-1α in human renal allograft biopsies. *J Am Soc Nephrol* 18: 343-351, 2007.
37. **Rosenberger C, Rosen S, Paliege A, and Heyman SN**. Pimonidazole adduct immunohistochemistry in the rat kidney: Detection of tissue hypoxia. *Methods Mol Biol* 466: 161-174, 2009.
38. **Sadowski EA, Djamali A, Wentland AL, Muehrer RJ, Becker BN, Grist TM, and Fain SB**. Blood oxygen level-dependent and perfusion magnetic resonance imaging: Detecting differences in oxygen bioavailability and blood flow in transplanted kidney. *Magn Reson Imaging* 28: 56-64, 2010.
39. **Schodel J, Klanke B, Weidemann A, Buchholz B, Bernhardt WM, Bertog M, Amann K, Korbmacher C, Wiesener M, Warnecke C, Kurtz A, Eckardt KU, and Willam C**. HIF-prolyl hydroxylases in the rat kidney: physiologic expression patterns and regulation in acute kidney injury. *Am J Pathol* 174: 1663-1674, 2009.
40. **Shapiro SS, and Wilk MB**. An analysis of variance test for normality (complete samples). *Biometrika* 52: 591-611, 1965.
41. **Siegemund M, van Bommel J, Stegenga ME, Studer W, van Iterson M, Annaheim S, Mebazaa A, and Ince C**. Aortic cross-clamping and reperfusion in pigs reduces microvascular oxygenation by altered systemic and regional blood flow distribution. *Anesth Analg* 111: 345-353, 2010.
42. **Vinuesa E, Hotter G, Jung M, Herrero Fresneda I, Torras J, and Sola A**. Macrophage involvement in the kidney repair phase after ischaemia/reperfusion injury. *J Pathol* 214: 104-113, 2008.
43. **Welch WJ, Baumgartl H, and Lubbers DW, S.** Nephron pO_2 and renal oxygen usage in the hypertensive rat kidney. *Kidney Int* 59: 230-237, 2001.
44. **Zurlo G, Guo J, Takada M, Wenyi W, and Zhang Q**. New insights into protein hydroxylation and its important role in human diseases. *Biochim Biophys Acta* 1866: 208-220, 2016.

639 Table 1: Systemic and blood oxygen parameters of rats 24 h or 5 days after ischemia or sham-ischemia

	Sham, 24 h		Ischemia, 24 h		Sham, 5 days		Ischemia, 5 days		2-way ANOVA			Dichotomous comparison	
Parameter		**N**		**N**		**N**		**N**	P_{Tr}	P_{T}	P_{Tr*T}	**S1 Vs I1**	**S5 Vs I5**
Systemic													
Body weight after ischemia or sham-ischemia (g)	397.6 ± 23.8	10	378.2 ± 17.6	9	469.4 ± 14.9	7	364.5 ± 19.7	8	0.005	0.17	0.05	0.77	0.002
Kidney weight (g)	1.5 (1.3, 1.5)	10	1.5 (1.4, 1.6)	9	1.4 (1.4, 1.7)	7	2.2 (2.2, 2.8)	8	< 0.001	<0.001	0.04	0.92	< 0.001
Kidney weight (g/g BW)	3.6 (3.3, 4.1)	10	3.9 (3.7, 4.2)	9	3.3 (3.2, 3.5)	7	6.6 (5.4, 8.3)	8	< 0.001	0.16	< 0.001	0.55	0.002
Mean arterial blood pressure (mmHg)	118.3 (108.4, 140.4)	10	123.9 (108.7, 134.4)	9	116.9 (102.3, 118.7)	7	116.3 (87.2, 122.3)	8	0.59	0.07	0.79	0.86	0.93
Blood oximetry													
Arterial blood PO_2 (mmHg)	113.7 ± 6.1	10	89.2 ± 4.7	9	97.4 ± 5.0	7	100.7 ± 7.7	8	0.09	0.70	0.03	0.01	0.93
Hematocrit (%)	44.8 (41.9, 45.6)	10	38.5 (35.4, 40.3)	9	43.0 (41, 44.5)	7	42.1 (41.4, 43.3)	8	0.01	0.35	0.06	0.04	0.07
Arterial blood SO_2 (%)	98.3 (97.1, 99.0)	10	96.5 (92.3, 97.5)	9	96.5 (94, 97.5)	7	97.5 (96.6, 98.5)	8	0.36	0.80	0.003	0.02	0.22
Renal oxygen delivery (µmol/min)	30.5 ± 2.7	10	21.7 ± 2.4	9	29.7 ± 5.5	7	20.8 ± 2.9	8	0.03	0.95	0.99	0.06	0.28
Renal oxygen delivery (nmol/min/g BW)	80.5 ± 2.7	10	57.7 ± 5.6	9	64.3 ± 12.7	7	56.5 ± 6.8	8	0.20	0.60	0.60	0.10	0.82
Renal oxygen consumption (µmol/min)	2.9 (1.1, 6.0)	6	1.1 (0.7, 2.7)	7	2.6 (1.8, 4.1)	7	1.4 (0.9, 2.1)	8	0.04	0.99	0.99	0.30	0.06
Renal oxygen consumption (nmol/min/g BW)	8.3 ± 2.8	6	4.1 ± 1.1	7	6.1 ± 1.2	7	3.8 ± 0.6	8	0.08	0.70	0.80	0.30	0.20
Fractional extraction O_2 (%)	10.1 (6.0, 17.8)	6	5.1 (3.3, 11.7)	7	7.9 (7.1, 14.4)	7	6.9 (4.7, 8.2)	8	0.11	0.95	0.70	0.44	0.51

Normality of the data was assessed using the Shapiro-Wilk test. Data that did not violate normality are expressed as mean ± standard error of the mean while data that violated normality are expressed as median (25th percentile, 75th percentile). P_{Tr}, P_T and P_{Tr*T} are the outcomes of 2 way analysis of variance (ANOVA) with factors treatment (Tr) and time (T) for data that did not violate normality. For data that violated normality, an ANOVA on ranking was performed instead. Dichotomous comparisons of continuous variables were made using Student's t-test for data that did not violate normality. For data that violated normality, a Mann-Whitney U-test was performed for dichotomous comparisons. P-values for dichotomous comparisons were conservatively adjusted using the Dunn-Sidak correction with k=2 to account for the fact that comparisons were made at 24 h and 5 days. BW: body weight, S1: 24 h after sham-ischemia, I1: 24 h after ischemia and reperfusion, S5: 5 days after sham-ischemia, I5: 5 days after ischemia and reperfusion.

640
641 Table 2: Renal hemodynamic of rats 24 h or 5 days after ischemia or sham-ischemia
642

	Sham, 24 h		**Ischemia, 24 h**		**Sham, 5 days**		**Ischemia, 5 days**		**2-way ANOVA**			**Dichotomous comparison**	
Parameter		**N**		**N**		**N**		**N**	**P_{Tr}**	**P_T**	**P_{Tr*T}**	**S1 Vs I1**	**S5 Vs I5**
Renal blood flow (ml/min)	3.5 ± 2.9	10	3.0 ± 0.4	9	3.6 ± 0.7	7	2.4 ± 0.3	8	0.13	0.83	0.68	0.55	0.29
Renal blood flow (µl/min/g BW)	9.09 ± 0.98	10	7.93 ± 0.79	9	7.71 ± 1.59	7	6.65 ± 0.78	8	0.30	0.21	0.96	0.60	0.81
Renal plasma flow (ml/min)	1.7 (1.5, 2.1)	10	1.7 (1.4, 2.0)	9	1.6 (1.5, 3.0)	7	1.6 (0.9, 1.9)	8	0.42	0.65	0.87	0.36	0.51
Renal plasma flow (µl/min/g BW)	5.1 ± 0.6	10	4.9 ± 0.5	9	4.4 ± 0.9	7	3.8 ± 0.4	8	0.77	0.31	0.94	0.96	0.80
Glomerular filtration rate (ml/min)	0.8 (0.7, 1.2)	10	0.001 (0, 0.008)	9	1.0 (0.5, 1.8)	7	0.07 (0.01, 0.4)	9	< 0.001	0.17	0.11	< 0.001	0.14
Glomerular filtration rate (nl/min/g BW)	2400 (1520, 2960)	10	3.3 (0, 2.2)	9	2110 (1040, 3470)	7	190 (27, 1080)	8	< 0.001	0.18	0.03	< 0.001	0.20
Urine flow (µl/min)	7.0 ± 1.0	10	1.0 ± 0.5	9	10.0 ± 4.0	7	6.0 ± 2.0	8	0.01	0.09	0.99	0.001	0.36
Urine flow (nl/min/g BW)	16.0 (10.0, 28.0)	10	2.2 (0, 5.5)	9	17.0 (13.0, 25.0)	7	15 (1.1, 39.0)	8	0.04	0.05	0.06	0.002	0.66
Sodium excretion (µmol/min)	0.4 (0.2, 1.0)	9	0 (0, 0.18)	9	0.20 (0.2, 0.6)	7	0.20 (0.1, 0.3)	8	0.004	0.46	0.09	0.003	0.38
Sodium excretion (nmol/min/g BW)	1.0 (0.5, 2.1)	9	0 (0, 0.47)	9	0.5 (0.36, 1.3)	7	0.6 (0.35, 0.71)	8	0.02	0.53	0.05	0.01	0.90

Sodium reabsorption (µmol/min)	111.9 (93.6, 170.2)	9	0.17 (0, 1.0)	9	138.3 (63.3, 250.4)	7	8.75 (1.5, 52.0)	8	< 0.001	0.2	0.15	< 0.001	0.14
Sodium reabsorption (nmol/min/g BW)	307.5 (204.7, 427.6)	9	0.46 (0, 2.7)	9	310 (143.6, 479.3)	7	25.7 (3.6, 153.1)	8	< 0.001	0.18	0.03	< 0.001	0.20
Filtration fraction (%)	46.9 (34.1, 69.8)	10	0.1 (0, 0.5)	9	48.5 (29.7, 60.5)	7	7.0 (0.6, 21.7)	8	< 0.001	0.13	0.02	< 0.001	0.20

Normality of the data was assessed using the Shapiro-Wilk test. Data that did not violate normality are expressed as mean ± standard error of the mean while data that violated normality are expressed as median (25th percentile, 75th percentile). P_{Tr}, P_T and P_{Tr*T} are the outcomes of 2 way analysis of variance (ANOVA) with factors treatment (Tr) and time (T) for data that did not violate normality. For data that violated normality, an ANOVA on ranking was performed instead. Dichotomous comparisons of continuous variables were made using Student's t-test for data that did not violate normality. For data that violated normality, a Mann-Whitney U-test was performed for dichotomous comparisons. P-values for dichotomous comparisons were conservatively adjusted using the Dunn-Sidak correction with k=2 to account for the fact that comparisons were made at 24 h and 5 days. BW: body weight, S1: 24 h after sham-ischemia, I1: 24 h after ischemia and reperfusion, S5: 5 days after sham-ischemia, I5: 5 days after ischemia and reperfusion.

Figure 1: Temporal changes of inner medullary tissue PO_2 following renal ischemia or sham ischemia. Values are mean ± SEM for rats subjected to either an hour of sham (n=5) or bilateral renal ischemia (n=7). Tissue PO_2, assessed as current through the carbon paste electrode, was recorded before (day -1) and after (days 0-5) surgery. Current was averaged over 24 h period and is expressed as a percentage of its mean value on to the day before the surgery (day -1). $P_{Treatment}$, P_{Time} and $P_{Treatment*Time}$ are the outcomes of a 2-way repeated measures analysis of variance with factors treatment and time. * denotes $P \leq 0.05$ for specific comparisons between the two treatment groups at each time point using Student's unpaired t-test, without correction for multiple comparisons.

Figure 2: Assessment of tissue PO_2 by Clark electrode. The electrode was first inserted 2 mm into the cortex at 6 random sites across the left kidney. In panel A, multiple measurements are shown for each rat, with the various rats represented by different symbols. Filled symbols represent rats subjected to renal ischemia (n=9 at 24 h and n=8 at 5 days) while open symbols represent rats subjected to sham ischemia (n=10 at 24 h and n=7 at 5 days). Measurements of cortical tissue PO_2 for each rat were averaged and are presented as the between rat mean ± SEM in (B). In panel B, P_{Tr}, P_T and P_{Tr*T} are the outcomes of a 2-way analysis of variance (ANOVA) with factors treatment and time. P-values above each pair of columns and error bars show the outcomes of Student's unpaired t-test conservatively adjusted using the Dunn-sidak correction with k = 2 to account for the fact that comparisons were made at 24 h and 5 days. A tissue PO_2 profile with depth was established by advancing the electrode from the cortical surface at 1 mm increments, up to 10 mm into the left kidney either 24 h (C) or 5 days (D) following recovery from either ischemia or sham-ischemia. Symbols and error bars are the mean ± SEM for rats subjected to either an hour of sham (open circles) or bilateral renal ischemia (closed circles). In panels C and D, P_D, P_{Tr} and P_{D*Tr} are the outcomes of 2-way repeated measures ANOVA with factors depth and treatment. * denotes $P \leq 0.05$ and is the outcome of Student's unpaired t-test without correction for multiple comparisons

Figure 3: Pimonidazole adduct immunohistochemistry of renal sections 24 h following recovery from bilateral renal ischemia or sham-ischemia. Images are typical of the cortical, outer and inner medullary region of the 6 kidneys examined in each group.

Figure 4: Pimonidazole adduct immunohistochemistry of renal sections 5 days following recovery from bilateral renal ischemia or sham surgery. Images are typical of the cortical, outer and inner medullary region of the 6 kidneys examined in each group.

Figure 5: **Expression of HIF proteins after bilateral renal ischemia or sham ischemia.** Immunoblots for HIF-1α (A-C) and HIF-2α (D-F) of tissue extracts from the cortex, outer and inner medulla of the left kidneys of rats 24 h and 5 days following recovery from either sham-ischemia (open circles) or bilateral renal ischemia (closed circles); n = 6 per group. Panel G shows a typical image of the gel following electrophoresis and panel H reflects a typical image of the nitrocellulose membrane following transfer. Values are expressed as median (25^{th} percentile, 75^{th} percentile). Paired comparisons were performed using the Mann-Whitney U-test. Because paired comparisons were made at two time points, P-values were conservatively adjusted using the Dunn-Sidak method with k = 2. P_{Tr}, P_T and P_{Tr*T} are the outcomes of 2 way analysis of variance on ranking with the factors treatment and time. AU: arbitrary unit, S1: 24 h after sham-ischemia, S5: 5 days after sham-ischemia, I1: 24 h after ischemia, I5: 5 days after ischemia

Figure 6: **mRNA expression of *HIF-1α, HIF-2α, VEGF-α and HO-1*.** Expression of *HIF-1α, HIF-2α, VEGF-α and HO-1* are presented as relative to that of control animals. Values are expressed as mean ± SEM and * denotes $P < 0.05$ for specific comparisons between the two treatment groups at each time point using Student's unpaired t-test.

Figure 7: **Collagen deposition in kidneys of rats.** The percentage areas of interstitial fibrosis relative to the areas of the cortex, outer and inner medulla are shown for rats 24 h and 5 days after recovery from either sham-ischemia or bilateral renal ischemia (IR), n = 6 per group. Values are expressed as mean ± SEM. Paired comparisons were performed using Student's unpaired t-test (*$P \leq 0.05$). Because paired comparisons were made at two time points, P-values were conservatively adjusted using the Dunn-Sidak method with k = 2. P_{Tr}, P_T and P_{Tr*T} are the outcomes of 2 way analysis of variance with the factors treatment (Tr) and time (T).

Figure 8: Indicators of renal dysfunction. Plasma concentrations of urea (A) and creatinine (B) and the urinary albumin to creatinine ratio (C) are shown for rats 24 h and 5 days after sham-ischemia (open circles) or bilateral renal ischemia (closed circles), n = 6 per group. Values are expressed as median (25^{th} percentile, 75^{th} percentile). Paired comparisons were performed using the Mann-Whitney U-test. Because paired comparisons were made at two time points, P-values were conservatively adjusted using the Dunn-Sidak method with k = 2. P_{Tr}, P_T and P_{Tr*T} are the outcomes of 2 way analysis of variance on ranking with the factors treatment (Tr) and time (T).

Figure 1

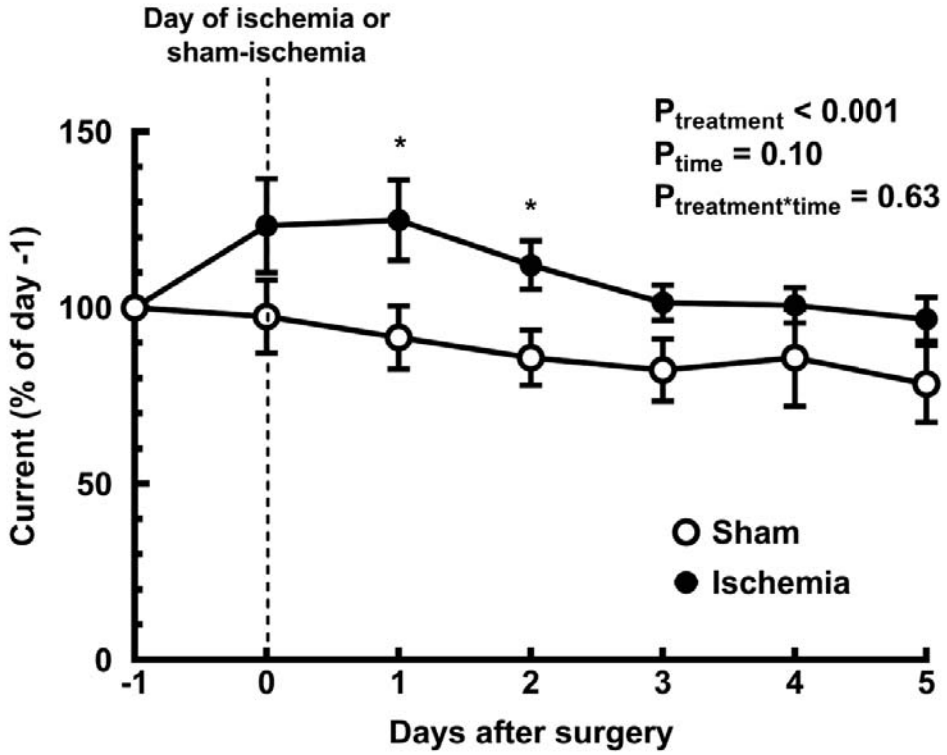
Day of ischemia or sham-ischemia
$P_{treatment} < 0.001$
$P_{time} = 0.10$
$P_{treatment*time} = 0.63$
*
*
150
100
50
0
Current (% of day -1)
-1
0
1
2
3
4
5
Days after surgery
Sham
Ischemia

Figure 2

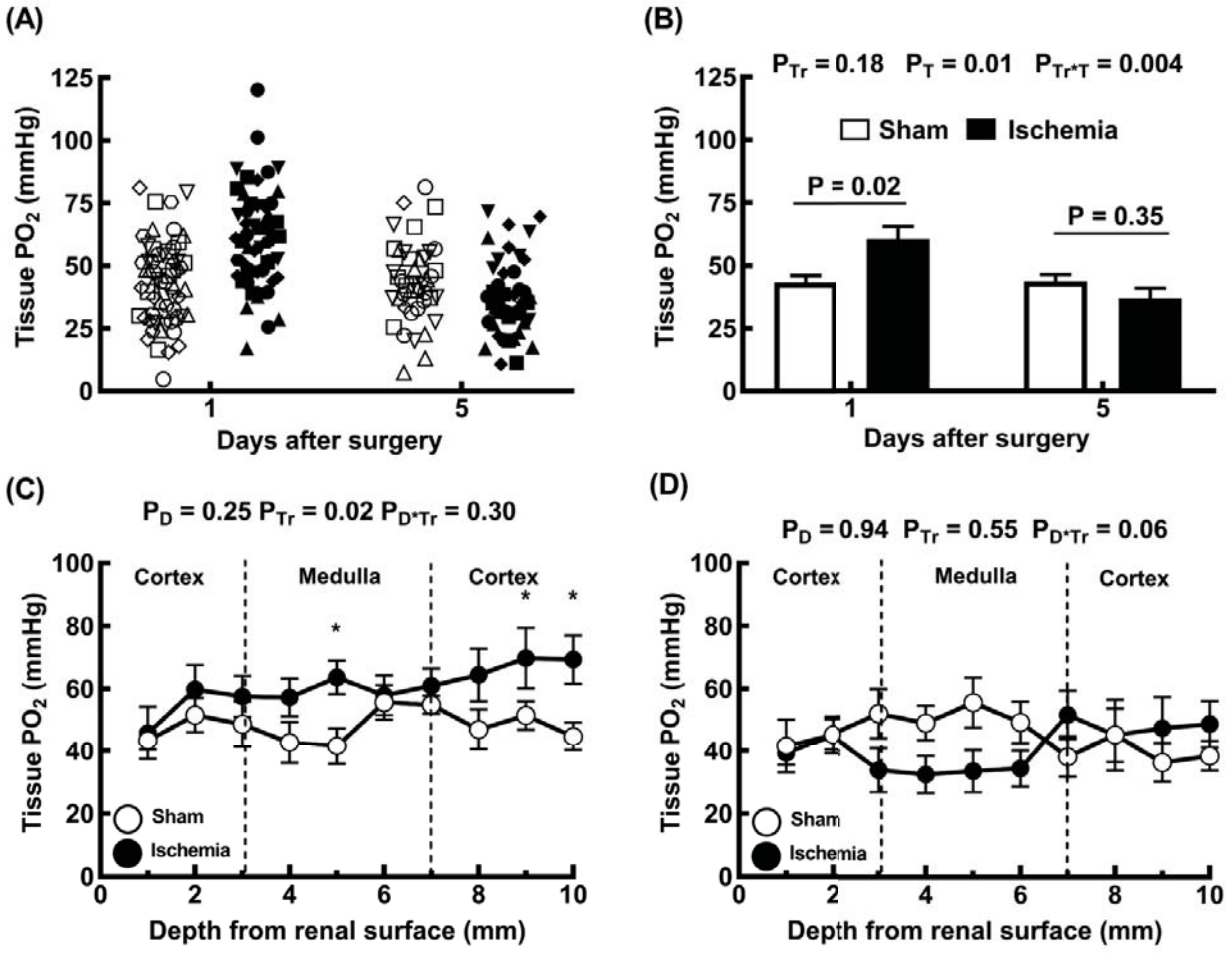
(A)
Tissue PO_2 (mmHg)
125
100
75
50
25
0
1
5
Days after surgery
(B)
P_{Tr} = 0.18 P_T = 0.01 P_{Tr*T} = 0.004
Sham
Ischemia
P = 0.02
P = 0.35
Tissue PO_2 (mmHg)
Days after surgery
(C)
P_D = 0.25 P_{Tr} = 0.02 P_{D*Tr} = 0.30
Cortex
Medulla
Cortex
Sham
Ischemia
Tissue PO_2 (mmHg)
Depth from renal surface (mm)
(D)
P_D = 0.94 P_{Tr} = 0.55 P_{D*Tr} = 0.06
Cortex
Medulla
Cortex
Sham
Ischemia
Tissue PO_2 (mmHg)
Depth from renal surface (mm)

Figure 3

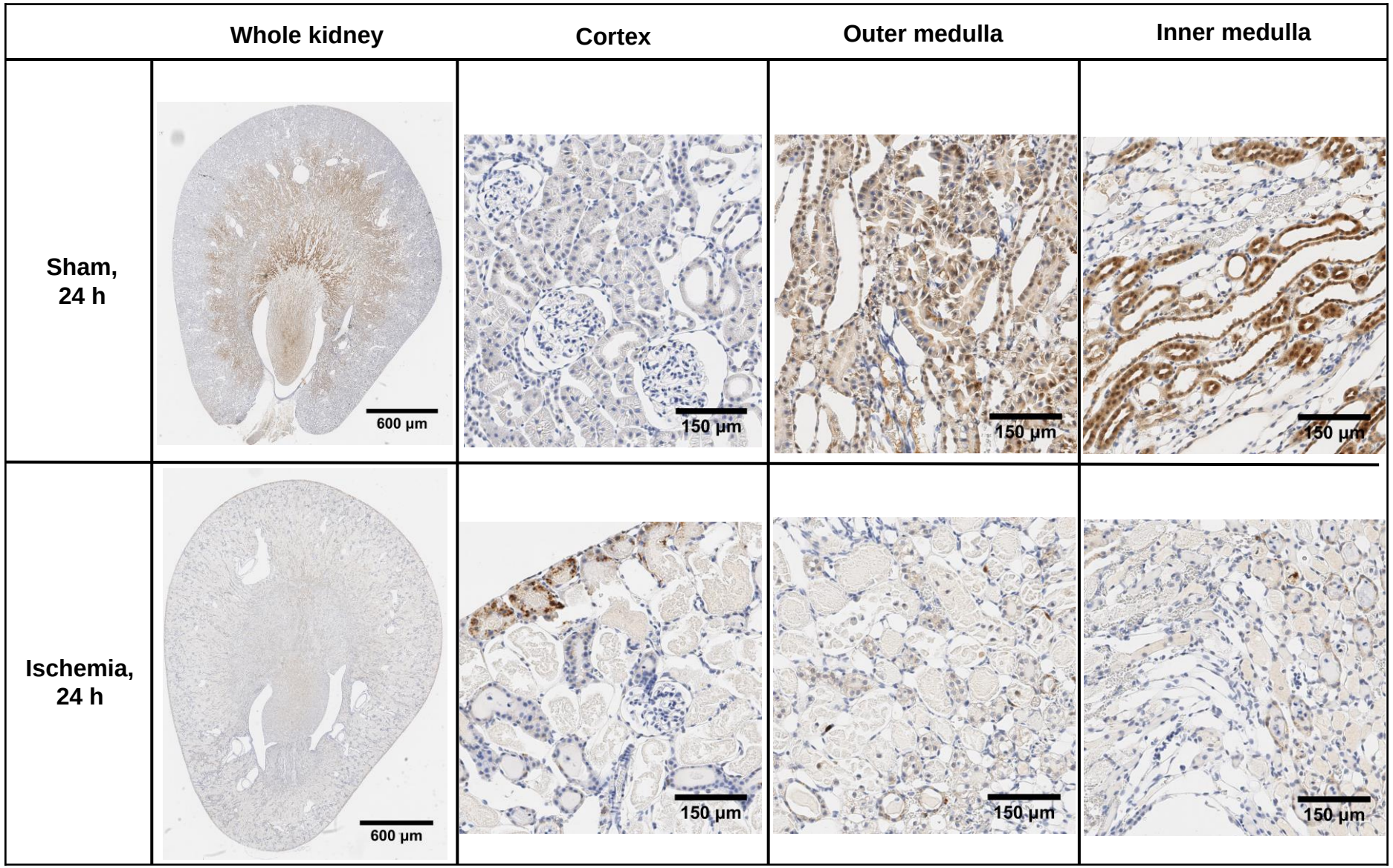
Whole kidney
Cortex
Outer medulla
Inner medulla
Sham, 24 h
Ischemia, 24 h
600 µm
150 µm
600 µm
150 µm
150 µm
150 µm

Figure 4

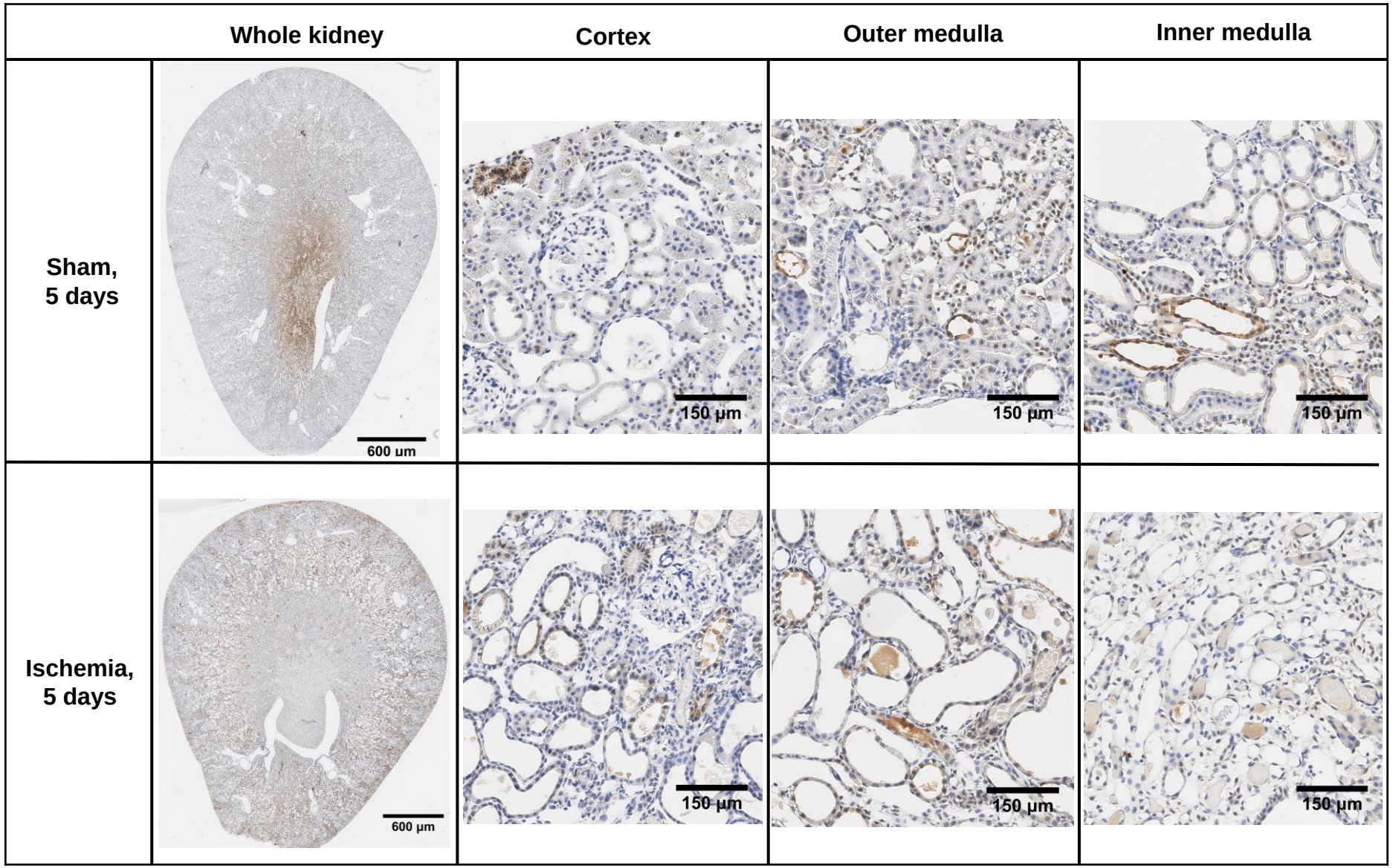
Whole kidney
Cortex
Outer medulla
Inner medulla
Sham,
5 days
Ischemia,
5 days
600 µm
150 µm
600 µm
150 µm
150 µm
150 µm
150 µm

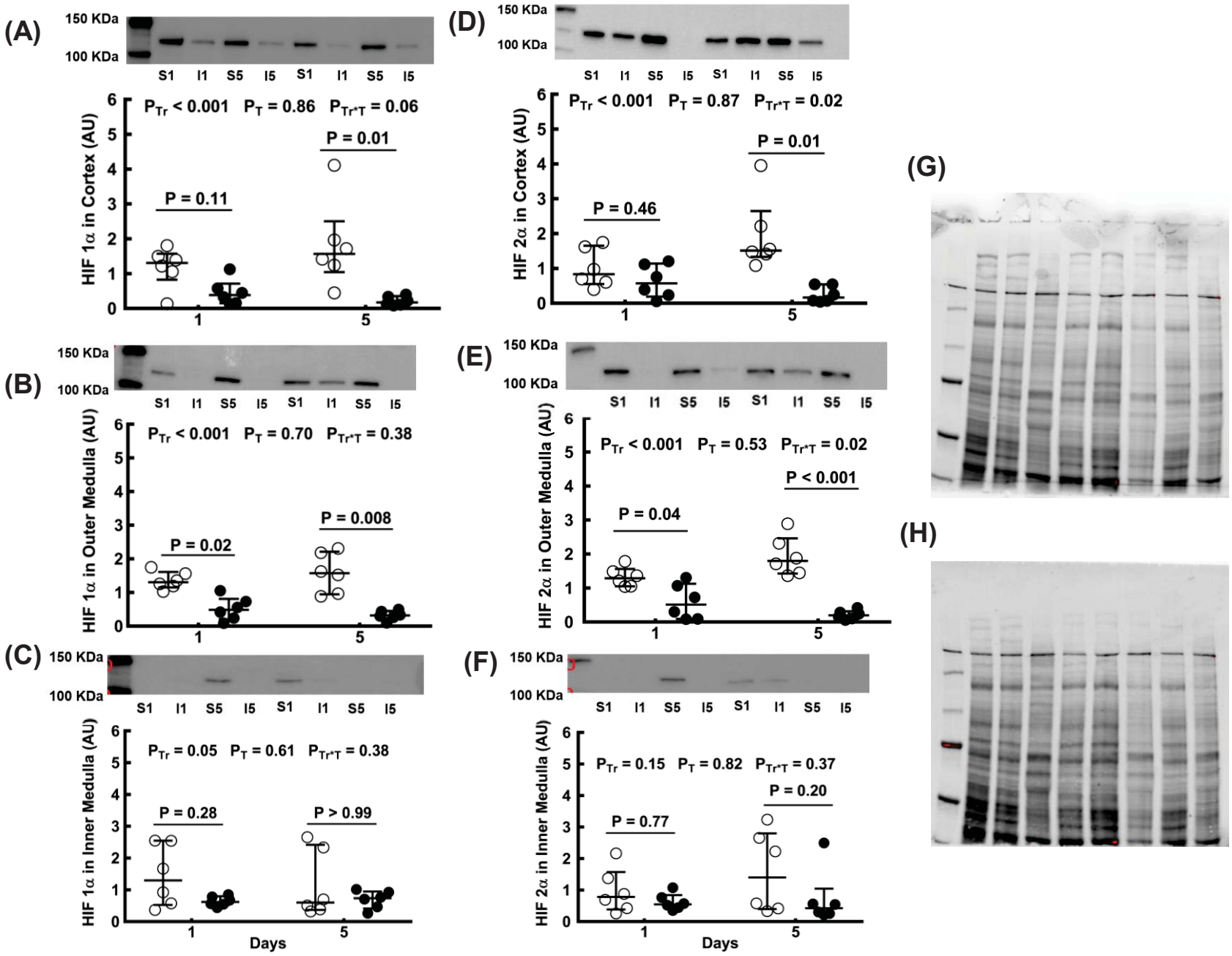
(A)
150 KDa
100 KDa
S1 I1 S5 I5 S1 I1 S5 I5
HIF 1α in Cortex (AU)
P_{Tr} < 0.001 P_T = 0.86 P_{Tr*T} = 0.06
P = 0.11
P = 0.01
(B)
150 KDa
100 KDa
S1 I1 S5 I5 S1 I1 S5 I5
HIF 1α in Outer Medulla (AU)
P_{Tr} < 0.001 P_T = 0.70 P_{Tr*T} = 0.38
P = 0.02
P = 0.008
(C)
150 KDa
100 KDa
S1 I1 S5 I5 S1 I1 S5 I5
HIF 1α in Inner Medulla (AU)
P_{Tr} = 0.05 P_T = 0.61 P_{Tr*T} = 0.38
P = 0.28
P > 0.99
Days
(D)
150 KDa
100 KDa
S1 I1 S5 I5 S1 I1 S5 I5
HIF 2α in Cortex (AU)
P_{Tr} < 0.001 P_T = 0.87 P_{Tr*T} = 0.02
P = 0.46
P = 0.01
(E)
150 KDa
100 KDa
S1 I1 S5 I5 S1 I1 S5 I5
HIF 2α in Outer Medulla (AU)
P_{Tr} < 0.001 P_T = 0.53 P_{Tr*T} = 0.02
P = 0.04
P < 0.001
(F)
150 KDa
100 KDa
S1 I1 S5 I5 S1 I1 S5 I5
HIF 2α in Inner Medulla (AU)
P_{Tr} = 0.15 P_T = 0.82 P_{Tr*T} = 0.37
P = 0.77
P = 0.20
Days
(G)
(H)

Figure 6

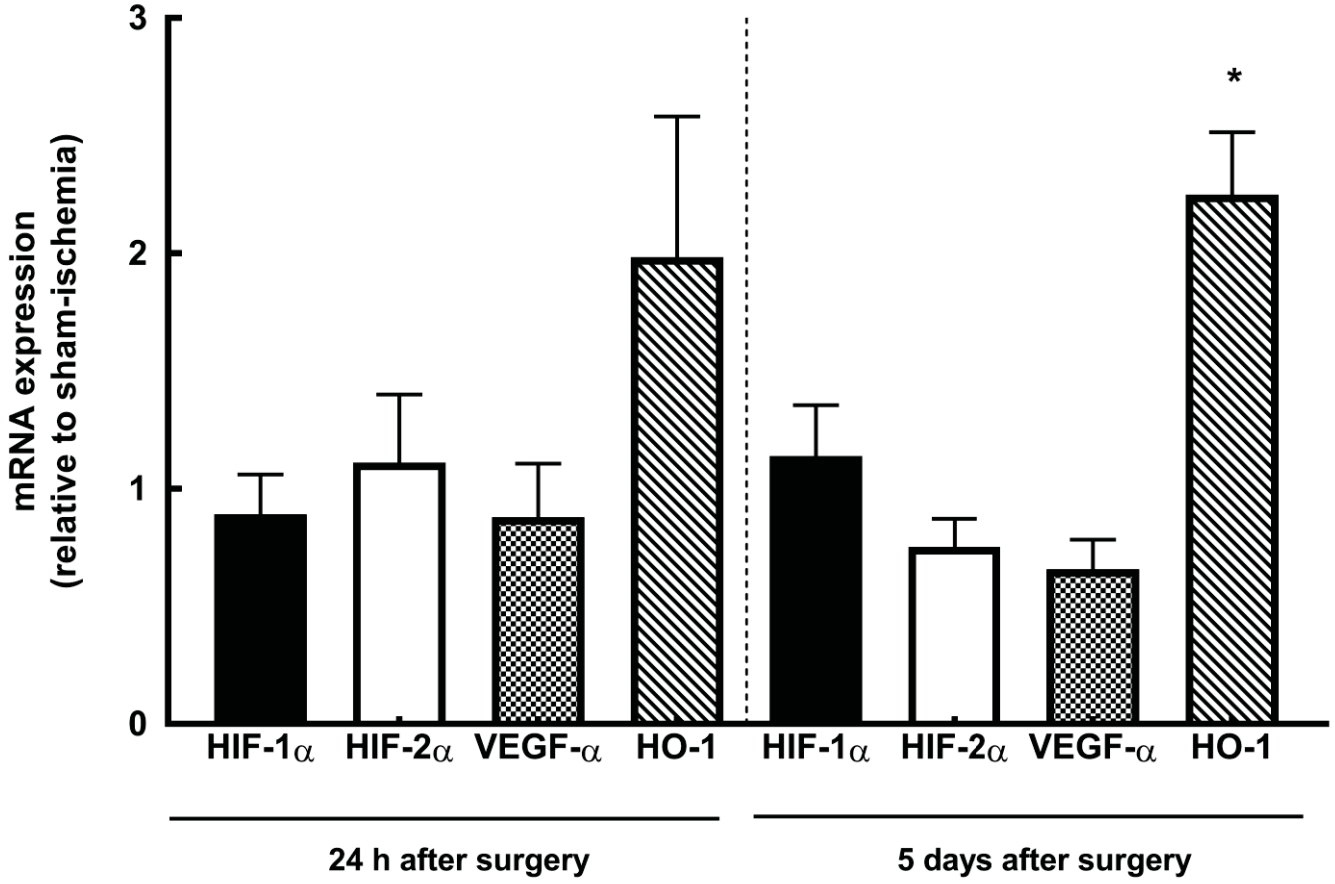
mRNA expression
(relative to sham-ischemia)
3
2
1
0
*
HIF-1α
HIF-2α
VEGF-α
HO-1
HIF-1α
HIF-2α
VEGF-α
HO-1
24 h after surgery
5 days after surgery

Figure 7

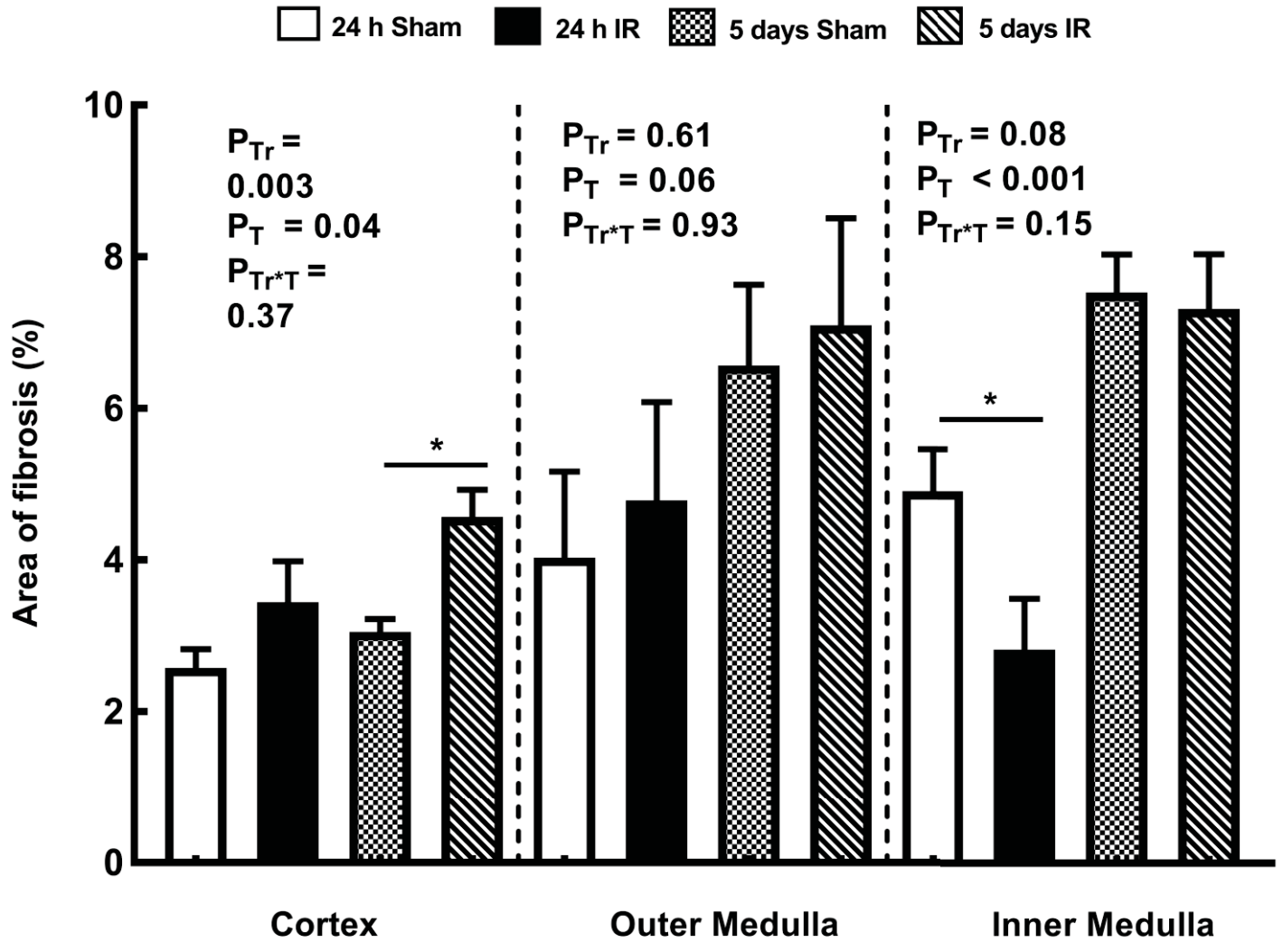
24 h Sham
24 h IR
5 days Sham
5 days IR
Area of fibrosis (%)
10
8
6
4
2
0
P_{Tr} = 0.003
P_T = 0.04
P_{Tr*T} = 0.37
*
P_{Tr} = 0.61
P_T = 0.06
P_{Tr*T} = 0.93
P_{Tr} = 0.08
P_T < 0.001
P_{Tr*T} = 0.15
*
Cortex
Outer Medulla
Inner Medulla

Figure 8

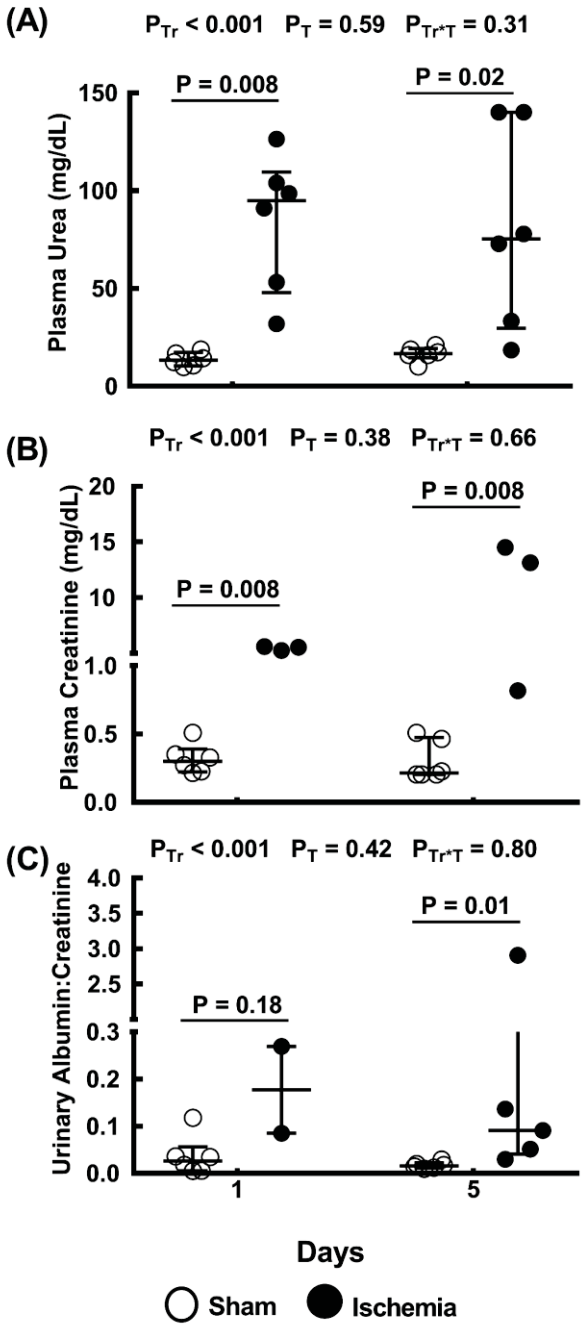
(A)
P_{Tr} < 0.001 P_T = 0.59 P_{Tr*T} = 0.31
P = 0.008
P = 0.02
Plasma Urea (mg/dL)
150
100
50
0
(B)
P_{Tr} < 0.001 P_T = 0.38 P_{Tr*T} = 0.66
P = 0.008
P = 0.008
Plasma Creatinine (mg/dL)
20
15
10
1.0
0.5
0.0
(C)
P_{Tr} < 0.001 P_T = 0.42 P_{Tr*T} = 0.80
P = 0.01
P = 0.18
Urinary Albumin:Creatinine
4.0
3.5
3.0
2.5
0.3
0.2
0.1
0.0
1
5
Days
Sham
Ischemia